




Cite this: *Chem. Commun.*, 2018, 54, 13670

Received 1st November 2018,
Accepted 7th November 2018

DOI: 10.1039/c8cc08673g

rsc.li/chemcomm

Diverse supramolecular structures self-assembled by a simple aryl chloride on Ag(111) and Cu(111)[†]

Chen-Hui Shu,[‡] Shao-Ze Zhang,[‡] Cheng-Xin Wang, Jian-Le Chen, Yan He, Ke-Ji Shi and Pei-Nian Liu *

Diverse self-assembled structures were obtained on Cu(111) and Ag(111) surfaces by using a simple and small 4,4''-dichloro-1,1':4',1''-terphenyl molecule. Surprisingly, a complicated supramolecular self-assembled vortex structure, composed of 15 molecules in a large unit, was realized through the collaboration of hydrogen bonding and halogen bonding.

Engineering of two-dimensional (2D) supramolecular self-assemblies has attracted widespread interest over the past few decades owing to the resulting systems' electrical and physical properties.¹ Recent progress in the fabrication of complicated supramolecular assembled structures with multi-molecules has been achieved in many aspects, such as the construction of hierarchic structures,^{1c,2} the transformation of chirality,³ *etc.* However, the construction of complicated supramolecular self-assembled structures using a simple molecule with one type of functional group has been rarely investigated,⁴ although such an approach would provide a unique chance to investigate the detailed assembly process.

Studies of halogenated molecules based on various experimental methods have demonstrated that the building blocks are interconnected to each other through directional intermolecular interactions such as hydrogen bonding (HB), halogen bonding (XB), *etc.*⁵ HB and XB based 2D supramolecular self-assemblies have often been reported on metal surfaces with precursors containing I or Br at low annealing temperatures.^{1c,6} In general, the HB of chlorides (C-H...Cl) is stronger than HB of bromides and iodides,⁷ which may offer an opportunity to generate more stable and sophisticated structures *via* self-assembly. However, the sophisticated 2D supramolecular assembly engineering of aryl chlorides has rarely been studied on surfaces.⁸

For the self-assembly of halogenated precursors containing I or Br, the annealing process on metal surfaces often leads to C-X bond activation, which severely limits their application in achieving thermodynamic self-assembled structures.⁹ Compared with Ph-I (65 kcal mol⁻¹) and Ph-Br (80 kcal mol⁻¹), the bond dissociation energy of Ph-Cl (95 kcal mol⁻¹) is higher, and aryl chlorides are more stable than aryl bromides and iodides.¹⁰ The superior stability of the C-Cl bond makes aryl chlorides a good choice to investigate the intrinsic properties of self-assembly systems at higher annealing temperature, which would lead to more sophisticated surface nanostructures as the thermodynamic products.

We report here the investigations of the supramolecular self-assembly of 4,4''-dichloro-1,1':4',1''-terphenyl (DCTP) molecules (Fig. 1a) under ultrahigh vacuum (UHV) on the Ag(111) and Cu(111) surfaces. Diverse 2D supramolecular networks of DCTP have been obtained on the surfaces at room temperature (RT). Owing to the high chemical stability of C-Cl, a highly complicated chiral vortex structure composed of 15 DCTP molecules was generated after annealing at 373 K. The emergence of such a structure with a large unit cell using a simple and small molecule is potentially of significant interest in the field of 2D crystal engineering. Based on the scanning tunneling microscopy (STM) studies and density functional theory (DFT) calculations, the main driving force was identified as hydrogen bonds between the Cl and H atoms, which cooperate with the halogen bonds of the chlorines to construct the complex structures.

The molecular electrostatic potential (ESP) surface with the contour line of the DCTP molecule was calculated to elucidate its self-assembly behavior (Fig. 1b). The outer regions of the Cl and H atoms within a lower electron density behave as electrophilic centers, the so-called σ -holes, which generate caps of depleted electrons upon elongation of the C-H or C-Cl bonds. The strength and orientation of the driving force in the self-assembly system, including C-H...Cl HB, C-Cl...Cl XB, and other intermolecular interactions, can be predicted and explained by analyzing the magnitudes and positions of minima and maxima on the surface.

Shanghai Key Laboratory of Functional Materials Chemistry, State Key Laboratory of Chemical Engineering and School of Chemistry & Molecular Engineering, East China University of Science and Technology, 130 Meilong Road, Shanghai, 200237, China. E-mail: liupn@ecust.edu.cn

[†] Electronic supplementary information (ESI) available: Supplemental STM images and calculation results. See DOI: 10.1039/c8cc08673g

[‡] These two authors contributed equally to this work.

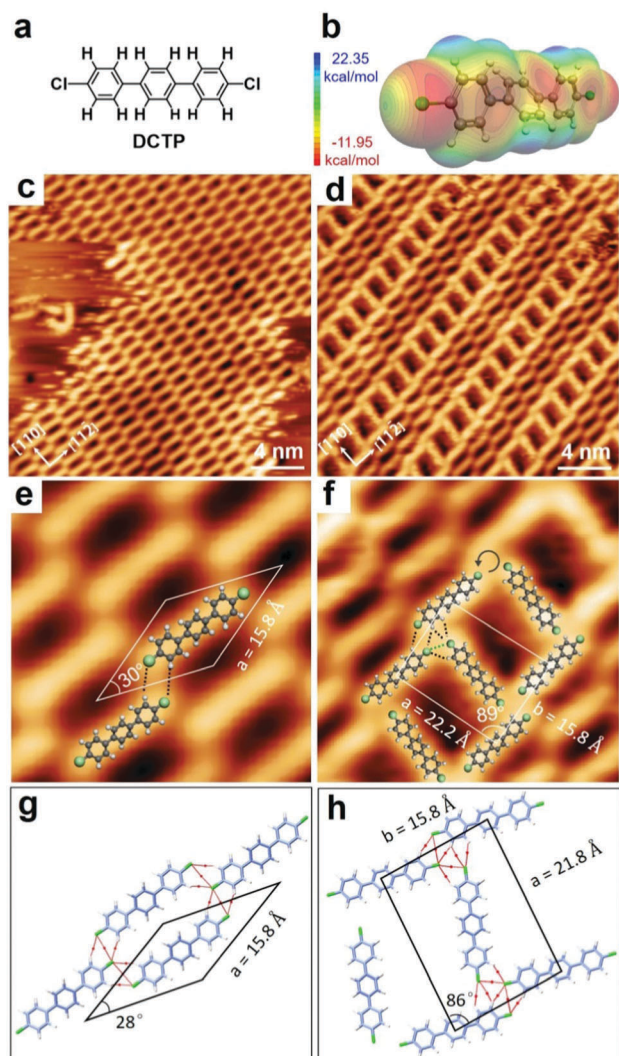


Fig. 1 DCTP molecules adsorbed on the Cu(111) surface at RT. (a) Chemical structure and (b) ESP surface of DCTP; (c) phase I; (d) phase II; (e) high-resolution image of phase I; (f) high-resolution image of phase II; molecular graphs obtained by calculations of (g) phase I and (h) phase II networks, where red dots represent the CPs, and red lines denote the bond paths. Scanning parameters of (c and e): $I = 0.07$ nA, $U = -1.68$ V; (d and f) $I = 0.07$ nA, $U = -1.22$ V.

DCTP molecules were deposited onto a clean surface of single-crystalline Cu(111) at RT under UHV conditions (base pressure: $\sim 2 \times 10^{-10}$ mbar). The DCTP molecules self-assembled into two coexisting phases, and their molecular models are overlaid in the STM images. The individual molecule can be identified as a stick with a length of 15 ± 0.2 Å, which is consistent with the DFT-predicted length of DCTP (14.9 Å). In self-assembled phase I, as shown in Fig. 1c, the DCTP molecules form stripes in a staggered arrangement. As shown in Fig. 1e, the unit cell contains one DCTP molecule, and the measured parameters are $a = 15.8 \pm 0.2$ Å, $\theta = 30 \pm 2^\circ$. In this structure, the measured distance of the C-H...Cl HBs based on the overlaid molecular modes (indicated by black dashed lines in Fig. 1e) is 3.1 ± 0.2 Å.

Another self-assembled phase, phase II (Fig. 1d) is more complicated; it consists of ladder-like structures separated by

two rows of molecules in a staggered arrangement. These two rows between the ladder structures are similar to the structure in Fig. 1c. In the ladder structure, the distances of two kinds of intermolecular bonds can be measured using the overlaid molecular models, including the C-H...Cl HB (3.0 ± 0.2 Å, black dashed line) and C-Cl...Cl XB (3.3 ± 0.2 Å, green dashed line). Interestingly, the windmill nodes in the ladder-like structure exhibit structural chirality (anticlockwise), although the DCTP molecules themselves do not have chirality. Another structural chirality with the clockwise nodes in the ladder-like structure can be found in Fig. S1 in the ESI.† When the sample was annealed to 323 K, the approximate ratio of phase I to phase II changed from 4:1 to 1:1, suggesting that phase I is kinetically favorable but phases I and II have similar thermodynamic properties. In addition, the calculated adsorption energies (E_{ads}) on Cu(111) per DCTP molecule for phases I and II are similar (-2.119 eV and -2.116 eV, Table 1), in agreement with the experimental results. Notably, annealing the sample to 353 K induced C-Cl bond activation and produced a C-Cu-C organometallic chain on the Cu(111) surface (see ESI,† Fig. S2a).^{10a}

Using the experimental lattice vectors, first-principles DFT calculations were performed on Cu(111) to determine the optimized structures of the DCTP networks in Fig. 1c. The optimized unit cell of $a = 15.8$ Å, $\theta = 28^\circ$ is shown in Fig. S3 and it matches the experimental measurements in Fig. 1e.

Considering that the intermolecular interactions are the main driving forces in the current self-assembled system, atoms-in-molecules (AIM) analysis was used to elucidate the bond properties of the interactions.¹¹ Critical points (CPs) were identified and are shown in Fig. 1g. The driving force for the self-assembly of phase I of DCTP on Cu(111) is found to be mainly HB (C-H...Cl) with a mean distance of 2.96 Å and a bonding energy of -27.5 meV (see Fig. S3 and Table S1, ESI†). Besides, an unconventional weak XB is also revealed by the CPs with an almost perpendicular angle (Fig. 1d).¹²

For the self-assembly of phase II in Fig. 1d, we simplified the DFT model by optimizing only the ladder-like structure on Cu(111) (see Fig. 1f and Fig. S4, ESI†). As shown in Fig. 1h, the CPs of the intermolecular bonds reproduce the binding mechanisms of the experimental observation in Fig. 1f. Two types of interactions are identified as the driving forces for the self-assembly: C-H...Cl HB and C-Cl...Cl XB. The distance of HB is approximately 3.15 Å, and the average bonding energy is -22.4 meV. The XBs show a mean bond distance of 3.83 Å and

Table 1 Summary of adsorption energies per DCTP molecule (E_{ads}), average bond length (d) and number of bonds in the four self-assembled models

	E_{ads} (eV)	Interactions	Number	Average d (Å)
Cu(111)-RT-I	-2.119	C-H...Cl	4	2.962
		C-Cl...Cl	2	4.061
Cu(111)-RT-II	-2.116	C-H...Cl	10	3.146
		C-Cl...Cl	4	3.826
Ag(111)-RT	-1.753	C-H...Cl	7	3.549
Ag(111)-373 K	—	C-H...Cl	35	3.039
		C-Cl...Cl	3	3.763

an average bonding energy of -26.1 meV (see Fig. S4 and Table S1 in the ESI†).

Next, we deposited DCTP molecules on a Ag(111) surface at RT. An STM image of the adsorbed DCTP molecules on Ag(111) shows a highly ordered self-assembled monolayer consisting of large paralleled stripes with a width of 16.8 ± 0.2 Å (Fig. 2a). The high-resolution STM image reveals a unit cell of $a = 15.5 \pm 0.2$ Å, $b = 16.8 \pm 0.2$ Å, $\theta = 87 \pm 2^\circ$ (Fig. 2c), two lines of molecules staggered arranged with an angle of $30^\circ \pm 2^\circ$ (Fig. 2c). Based on the overlaid molecular models, the intermolecular interaction of HB ($\text{C-H} \cdots \text{Cl}$) can be identified with the measured distances of $2.9\text{--}3.4 \pm 0.2$ Å.

Based on the DFT calculations, the corresponding assembled model of the DCTP molecules on Ag(111) was optimized with a unit cell of $a = 15.7$ Å, $b = 17.1$ Å, $\theta = 87^\circ$ (Fig. 2e and Fig. S5 in the ESI†), which is in reasonable agreement with the experimental measurements. According to the CP analysis shown in Fig. 2e, the main driving force for the formation of the self-assembly shown in Fig. 2c is identified as $\text{C-H} \cdots \text{Cl}$ HB with a mean distance of 3.02 Å and a bonding energy of -25 meV

(see Fig. S5 and Table S1 in the ESI†). Besides, some weak HBs between the stripes were revealed.

After the sample was annealed to 373 K, the strip phase of DCTP evolved to a new phase with vortex structures. We found two enantiomeric molecular phases with planar chirality for this vortex structure, the anticlockwise phase (Fig. 2b) and the clockwise phase (Fig. S6 in the ESI†). The close-up STM image shows that the individual molecule is still intact and the annealing process does not induce the C–Cl bond activation of DCTP on Ag(111) (Fig. 2d). In contrast, aryl bromides and aryl iodides are converted to organometallic products at this or even lower temperature.^{1c,13} It is noteworthy that the C–Cl bond was activated at 393 K to form a C–Ag–C organometallic chain (see the ESI,† Fig. S2b),^{10a} which demonstrates the remarkable effect of subtle temperature changes.

A careful analysis of this vortex structure demonstrates that the basic unit is a complicated self-assembly of 15 DCTP molecules. In the center of this self-assembled structure is a windmill core composed of three molecules (indicated by blue dashed frames in Fig. 2d); this bonding pattern is different from that in a previous study of the halogen-3 synthon because of the much longer distance (5.8 Å) between two chlorine atoms.¹⁴ According to the overlaid model of the triangular core structure, the measured distance of the $\text{C-H} \cdots \text{Cl}$ HB is 3.0 ± 0.2 Å (black dashed lines in Fig. 2d). Between every pair of molecules in the windmill core, there are four molecules and a total of 12 molecules are included in the three sections. One of the four molecules forms a $\text{C-Cl} \cdots \text{Cl}$ XB of 3.6 ± 0.2 Å (green dashed line) with the central molecule. Besides, there are many $\text{C-H} \cdots \text{Cl}$ HBs with a distance of $2.9\text{--}3.5 \pm 0.2$ Å. A line profile along the blue line in Fig. 2b demonstrates that the vortex structure appears a little higher than the outside area, which might be caused by the difference of the electronic local density of states.

The DFT calculations were performed under vacuum due to the limitation of the calculation resource to elucidate the driving forces and numerous interactions in this arranged vortex structure (Fig. 2f, Fig. S7 and Table S1 in the ESI†). In the center of this self-assembled structure, the windmill structure is composed of three molecules (indicated by a green dashed frame as **I**) that contact each other by forming six similar $\text{C-H} \cdots \text{Cl}$ HBs with a mean bond distance of 2.92 Å and a mean bond strength of -36.8 meV. Each molecule indicated by a red dashed frame as **II** inserts into the gap between every two molecules of the windmill core, forming one $\text{C-Cl} \cdots \text{Cl}$ XB (bond distance: 3.76 Å; bond strength: -24.8 meV) and one weak HB (bond distance: 3.32 Å; bond strength: -11.0 meV) with the adjacent two molecules. For the three molecules **III** indicated by a black dashed frame, each one inserts into the gap between molecules **I** and **II** as depicted in Fig. 2f. In total 10 HBs have been identified with a mean bond distance of 2.98 Å and a mean bond strength of -38.4 meV from the interactions of molecule **III** with the adjacent molecules **I** and **II**. As shown in Fig. 2f, the last six molecules **IV** without a frame arrange on both sides of the three molecules **I** to form the vortex structure. Every molecule **IV** forms two HBs with molecule **I** with a mean bond distance of 2.98 Å and a mean bond strength of -33.0 meV.

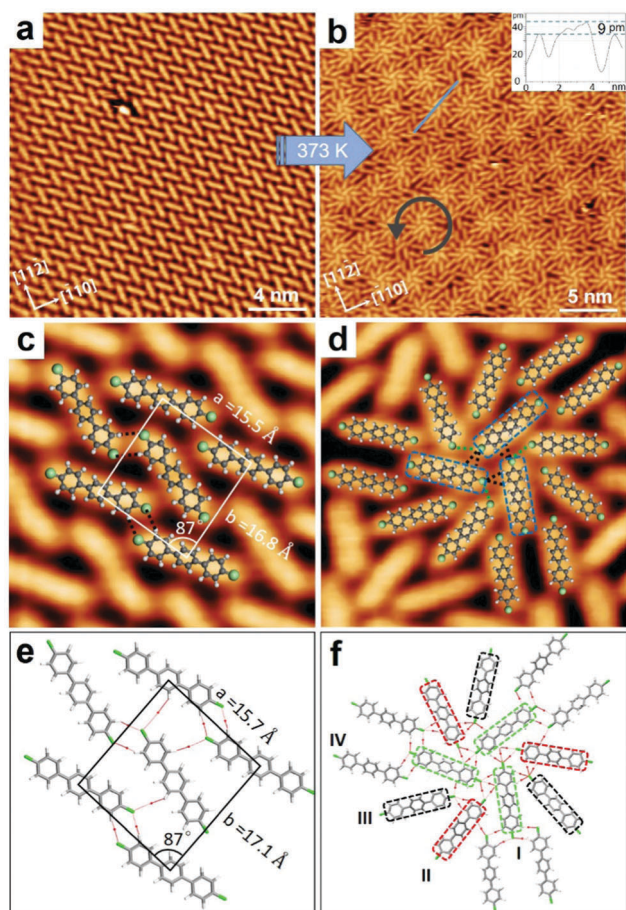


Fig. 2 DCTP molecules adsorbed on the Ag(111) surface. (a) DCTP deposited at RT; (b) DCTP after annealing at 373 K; (c) high-resolution image of (a); (d) high-resolution image of (b); (e and f) molecular graphs obtained by calculations of (c) and (d) networks, respectively, where red dots represent the CPs, and red lines denote the bond paths. Scanning parameters: (a and c) $I = 0.06$ nA, $U = -1.50$ V; (b and d) $I = 0.07$ nA, $U = 2.50$ V.

Notably, some HBs can also be identified between molecules **IV** with the adjacent molecule **II**.

As discussed above, 35 C–H...Cl HBs and 3 C–Cl...Cl XBs were identified in the optimized vortex structure (Table 1 and Table S1 in ESI†), demonstrating that HBs are the main driving force in the formation of the vortex structure, and XBs appear in the structure. Then, the vortex units self-assemble by intermolecular interactions to form the 2D supramolecular nanostructure.

To understand the effect of substrate on the emergence of different 2D assemblies, the adsorption energies per DCTP molecule on Cu(111) and Ag(111) were determined to be -2.12 eV (for both phases **I** and **II**) and -1.75 eV (for the structure obtained at RT), respectively. Therefore, the smaller adsorption energy of DCTP on Ag(111) enables the diverse adsorption directions to construct the complicated vortex structure.

We also investigated the self-assembly of molecule 1,1':4',1''-terphenyl on Ag(111) as a control experiment to elucidate the role of C–H...Cl in the assembly process. The results show a simply staggered self-assembly pattern, forming on the basis of a weak dispersion force (see the ESI,† Fig. S8). Therefore, the chlorine atoms in DCTP are crucial to generate HBs and XBs, which guide the formation of the elegant structures.

In summary, we have achieved several 2D supramolecular networks at RT on the Cu(111) and Ag(111) surfaces when simple and small aryl chloride DCTP was used as a precursor. Owing to the high chemical stability of the C–Cl bond, an interesting chiral vortex structure composed of 15 DCTP molecules was obtained on Ag(111) with intact DCTP molecules after annealing at 373 K. Through a combination of STM and DFT calculations, C–H...Cl hydrogen bonding was identified as the main driving force for the self-assembly owing to the strong electronegativity of chlorine, although halogen bonds also play important roles in the self-assembly of various structures. Our findings shed light on molecular engineering to tailor the on surface self-assembly of organic precursors to fabricate sophisticated structures.

This work was supported by the National Natural Science Foundation of China (Project No. 21672059 and 21561162003), the Program of the Shanghai Committee of Science and Technology (Project No. 18520760700) and the Eastern Scholar Distinguished Professor Program. The calculations were performed on TianHe-1 (A) at National Supercomputer Center in Tianjin.

Conflicts of interest

The authors declare no competing financial interests.

Notes and references

- (a) L. Bartels, *Nat. Chem.*, 2010, **2**, 87; (b) N. A. Wasio, R. C. Quardokus, R. P. Forrest, C. S. Lent, S. A. Corcelli, J. A. Christie, K. W. Henderson and S. A. Kandel, *Nature*, 2014, **507**, 86; (c) Y.-Q. Zhang, M. Paszkiewicz, P. Du, L. Zhang, T. Lin, Z. Chen, S. Klyatskaya, M. Ruben, A. P. Seitsonen, J. V. Barth and F. Klappenberger, *Nat. Chem.*, 2018, **10**, 296.
- (a) J. Liu, T. Chen, X. Deng, D. Wang, J. Pei and L.-J. Wan, *J. Am. Chem. Soc.*, 2011, **133**, 21010; (b) H. Spillmann, A. Dmitriev, N. Lin, P. Messina, J. V. Barth and K. Kern, *J. Am. Chem. Soc.*, 2003, **125**, 10725.
- (a) K. Tahara, H. Yamaga, E. Ghijsens, K. Inukai, J. Adisojoso, M. O. Blunt, S. De Feyter and Y. Tobe, *Nat. Chem.*, 2011, **3**, 714; (b) T. Chen, W.-H. Yang, D. Wang and L.-J. Wan, *Nat. Commun.*, 2013, **4**, 1389.
- D. Ćija, K. Seufert, D. Heim, W. Auwärter, C. Aurisicchio, C. Fabbro, D. Bonifazi and J. V. Barth, *ACS Nano*, 2010, **4**, 4936.
- (a) A. R. Voth, F. A. Hays and P. S. Ho, *Proc. Natl. Acad. Sci. U. S. A.*, 2007, **104**, 6188; (b) N. Oshrit, B. Joel and K. Vladimirov, *Angew. Chem., Int. Ed. Engl.*, 1997, **36**, 601; (c) E. Corradi, S. V. Meille, M. T. Messina, P. Metrangolo and G. Resnati, *Angew. Chem., Int. Ed.*, 2000, **39**, 1782; (d) C. B. Aakeröy, M. Fasulo, N. Schultheiss, J. Desper and C. Moore, *J. Am. Chem. Soc.*, 2007, **129**, 13772; (e) A. Priimagi, G. Cavallo, P. Metrangolo and G. Resnati, *Acc. Chem. Res.*, 2013, **46**, 2686.
- (a) K.-H. Chung, H. Kim, W. J. Jang, J. K. Yoon, S.-J. Kahng, J. Lee and S. Han, *J. Phys. Chem. C*, 2013, **117**, 302; (b) J. Eichhorn, T. Strunskus, A. Rastgo-Lahrood, D. Samanta, M. Schmitt and M. Lackinger, *Chem. Commun.*, 2014, **50**, 7680; (c) L. Grill, M. Dyer, L. Lafferentz, M. Persson, M. V. Peters and S. Hecht, *Nat. Nanotechnol.*, 2007, **2**, 687; (d) J. Shang, Y. Wang, M. Chen, J. Dai, X. Zhou, J. Kuttner, G. Hilt, X. Shao, J. M. Gottfried and K. Wu, *Nat. Chem.*, 2015, **7**, 389.
- (a) L. Brammer, E. A. Bruton and P. Sherwood, *Cryst. Growth Des.*, 2001, **1**, 277; (b) C. B. Aakeröy, T. A. Evans, K. R. Seddon and I. Pálkó, *New J. Chem.*, 1999, **23**, 145.
- (a) N. Seung-Kyun, J. J. Heum, J. W. Jun, K. Howon, L. Soon-Hyeong, L. M. Wook, L. Jinhwan, H. Seungwu and K. Se-Jong, *ChemPhysChem*, 2013, **14**, 1177; (b) K. J. Shi, X. Zhang, C. H. Shu, D. Y. Li, X. Y. Wu and P. N. Liu, *Chem. Commun.*, 2016, **52**, 8726; (c) P. H. Jacobse, A. van den Hoogenband, M.-E. Moret, R. J. M. Klein Gebbink and I. Swart, *Angew. Chem., Int. Ed.*, 2016, **55**, 13052.
- (a) M. Bieri, M. Treier, J. Cai, K. Ait-Mansour, P. Ruffieux, O. Groning, P. Groning, M. Kastler, R. Rieger, X. Feng, K. Mullen and R. Fasel, *Chem. Commun.*, 2009, 6919; (b) Q. Shen, J. H. He, J. L. Zhang, K. Wu, G. Q. Xu, A. T. S. Wee and W. Chen, *J. Chem. Phys.*, 2015, **142**, 101902; (c) X. Zhou, F. Bebensee, M. Yang, R. Bebensee, F. Cheng, Y. He, Q. Shen, J. Shang, Z. Liu, F. Besenbacher, T. R. Linderoth and K. Wu, *ACS Nano*, 2017, **11**, 9397; (d) S. Zint, D. Ebeling, T. Schlöder, S. Ahles, D. Mollenhauer, H. A. Wegner and A. Schirmeisen, *ACS Nano*, 2017, **11**, 4183.
- (a) K. J. Shi, D. W. Yuan, C. X. Wang, C. H. Shu, D. Y. Li, Z. L. Shi, X. Y. Wu and P. N. Liu, *Org. Lett.*, 2016, **18**, 1282; (b) G. Galeotti, M. Di Giovannantonio, J. Lipton-Duffin, M. Ebrahimi, S. Tebi, A. Verdini, L. Floreano, Y. Fagot-Revurat, D. F. Perepichka, F. Rosei and G. Contini, *Faraday Discuss.*, 2017, **204**, 453.
- (a) R. F. W. Bader, *Chem. Rev.*, 1991, **91**, 893; (b) I. Rozas, I. Alkorta and J. Elguero, *J. Am. Chem. Soc.*, 2000, **122**, 11154.
- A. Mukherjee, S. Tothadi and G. R. Desiraju, *Acc. Chem. Res.*, 2014, **47**, 2514.
- M. Ammon, T. Sander and S. Maier, *J. Am. Chem. Soc.*, 2017, **139**, 12976.
- Z. Han, G. Czap, C.-I. Chiang, C. Xu, P. J. Wagner, X. Wei, Y. Zhang, R. Wu and W. Ho, *Science*, 2017, **358**, 206.